THE JOURNAL OF PHYSICAL CHEMISTRY B

ARTICLE

pubs.acs.org/JPCB

Aggregation Behavior of Amino Acid Ionic Liquid Surfactants in Aqueous Media

K. Srinivasa Rao, Tejwant Singh, Tushar J. Trivedi, and Arvind Kumar*

Salt and Marine Chemicals Division, Central Salt and Marine Chemicals Research Institute, Council of Scientific and Industrial Research (CSIR), G. B. Marg, Bhavnagar 364002, India

Supporting Information

ABSTRACT: Self-aggregation of amino acid ionic liquid surfactants (AAILSs) in aqueous solution has been investigated through surface tension, conductivity, steady-state fluorescence, dynamic light scattering (DLS), and transmission electron microscopy (TEM). The critical aggregation concentration (cac) of AAILSs obtained from different techniques showed fairly good agreement. Surface tension measurements have been used to derive surface adsorption properties such as adsorption efficiency (pC_{20}), effectiveness of surface tension reduction (Π_{cac}), and minimum surface area per molecule (A_{min}) at the air−water interface. Temperature-dependent conductivity measurements have been used to obtain the degree of counterion binding (β), and the thermodynamic parameters such as standard free energy (ΔG_{agg}^0), enthalpy (ΔH_{agg}^0), and entropy (ΔS_{agg}^0) of aggregation. The aggregation number (N_{agg}) for various AAILSs has been derived by using the fluorescence quenching technique. Size of the aggregates has been obtained from DLS and TEM measurements. The aggregation properties of AAILSs have been analyzed as a function of structure of amino acids and compared with those of analogous ionic liquids (ILs) and conventional ionic surfactants. Surface activity of the AAILSs has been found superior to that of analogous ILs and conventional ionic surfactants of the same alkyl chain length.

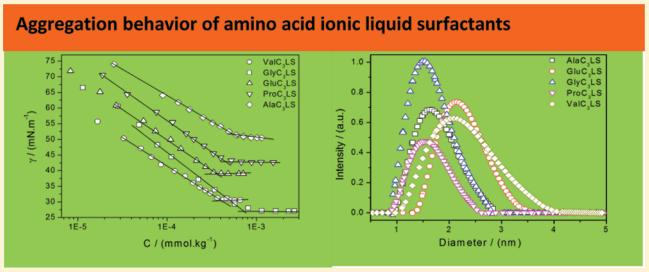

1. INTRODUCTION

Room temperature ionic liquids (ILs), due to their unique physical and chemical properties, have aroused great interest among scientific community. ILs have an edge over the conventional organic solvents in terms of very low vapor pressure, large liquid range, high thermal stability, nonflammability under ambient conditions, wide electrochemical window, and strong ability to dissolve many organic or inorganic solutes. Because of unique physicochemical properties, the ILs have been the focus of many scientific investigations.[1−10] Many of the ILs are emerging as novel surfactants due to the amphiphilic nature of their cation or anion, and have been explored for their aggregation behavior by many researchers including our own research group.[11−37] With the possibility of fine-tuning the amphiphilicity of ILs by changing the alkyl chain length or polarizability of the cation and anion one can generate specific self-assembled structures. The specific self-assembled structures of ILs can act as novel micellar catalyst, and can show a different or even improved templating behavior for the synthesis of nanostructured materials for different applications.[38−43] Therefore, the investigations on the self-assembling behavior of ILs as a novel class of surfactants are gaining momentum.

Earlier, we reported the synthesis and task specific applications of AAILSs.[44] The synthesized AAILSs were found to be advantageous in terms of higher water solubility, chiral properties, and biodegradability. AAILSs also showed better surface-active properties as compared to similar kind of conventional surfactants. In the present paper, a detailed study has been carried out on the aggregation behavior and thermodynamics of self-assembling of AAILs in the aqueous medium by using tensiometry and conductometry techniques. The micropolarity of the aggregates is usually studied from the steady-state fluorescence spectroscopy using pyrene as polarity probe.[11] Therefore, we recorded the pyrene fluorescence in the aqueous solutions of AAILSs and used the relative intensity of vibronic bands (I_1/I_3) to determine the cac of various AAILSs. Fluorescence quenching experiments were performed in order to obtain the aggregation number of AAILSs aggregates. Information about the size and shape of the IL aggregates was gathered from DLS and TEM methods.

In brief, we have characterized the surfactant properties of a new class of ionic liquid surfactants comprising amino acids and lauryl sulfate. Thermodynamics of aggregation has been discussed in detail and surface properties are compared with those of conventional surfactants or ILs having the same alkyl chain length. Results show that surface properties of AAILSs are superior to those of conventional surfactants and depend upon the structure of counterion amino acid. The reasons for the higher surface activity of AAILSs are discussed.

2. EXPERIMENTAL SECTION

2.1. Materials. Amino acids (L-glycine, L-alanine, L-valine, L-glutamic acid and L-proline) and sodium lauryl sulfate (SLS),

Received: August 9, 2011
Revised: September 26, 2011
Published: October 26, 2011

Scheme 1. Molecular Strzucture of Various Cations and Anion of the Synthesized AAILSs

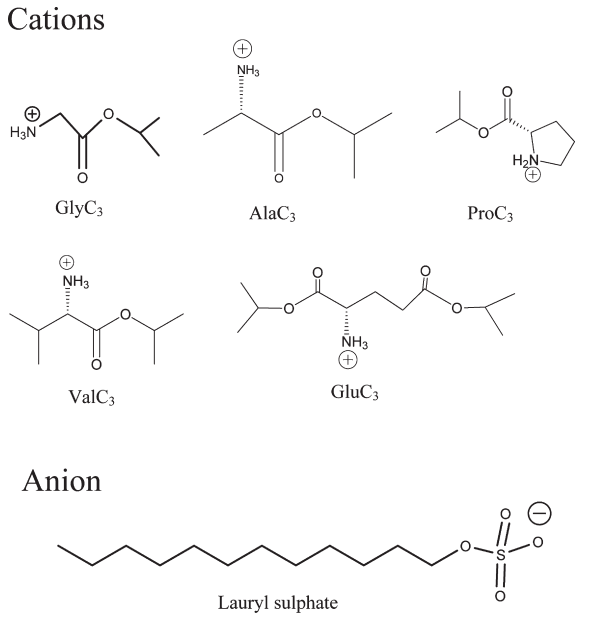

all having a purity of >0.99 mass fraction, were obtained from Sisco Research Laboratories Pvt. Ltd., Mumbai. The AAILSs were synthesized by adopting a simple strategy of esterification of amino acids and metathesis with sodium lauryl sulfate (SLS), as reported in our earlier communication.[44] In a brief procedure, the esterification of amino acids was carried out by either isopropyl alcohol or isobutyl alcohol. For the esterification, thionyl chloride was added slowly to isopropyl alcohol at 0 °C and then amino acids were added slowly. The reaction mixture was refluxed for 4 h. Thereafter, the solvent was concentrated in a rota-evaporator and crude amino acid ester hydrochloride was titurated with hexane at 0 °C. Pure crystals of amino acid ester hydrochlorides (AAECls) were obtained by recrystallization with methanol/hexane. AAILSs were prepared by dissolving equimolar amounts of AAECls and SDS in hot water. After the completion of reaction, water was removed under vacuum and the product was extracted by addition of dichloromethane. Since the trace amounts of water in ILs can have a dramatic effect on physical properties,[45,46] all the ILs were dried and degassed under vacuum at 60 °C for 2−3 days to remove water. Karl Fischer analysis of the samples indicated that the water content was reduced to less than 0.02% in all the liquids. The chloride content, measured by Vollhard's method, was found to be <0.01% in each liquid.[47] Structures of the synthesized AAILSs are shown in Scheme 1, and the chemical analysis of the compounds is given in the Supporting Information. Purity of the synthesized AAILSs determined from various techniques was ≥0.98 mass fraction. Henceforth, we will use general symbols to represent the AAILSs and use the number of carbon atoms to represent the alkyl groups of ester, say, proline propyl ester lauryl sulfate as, $ProC_3LS$. Aqueous solutions of AAILSs were prepared by weight using an analytical balance with a precision of ±0.0001 g (Denver Instrument APX-200) in degassed Millipore grade water.

2.2. Methods. *2.2.1. Tensiometry.* Surface tension measurements were carried out at 298.15 K using a DataPhysics DCAT II automated tensiometer employing the Wilhelmy plate method. AAILSs were added to water by weight and stirred for about 10 min

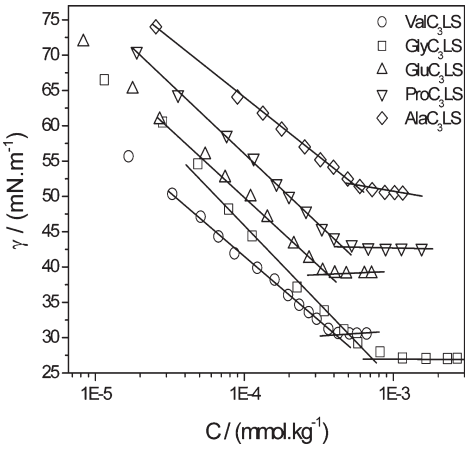

Figure 1. Surface tension (γ) as a function of concentration of various AAILSs at 298.15 K. The intersection of two straight lines depicts the cac. Data has been shifted vertically for better clarity.

for complete solubilization. Prior to measurements, the resultant solutions were kept for at least 10 min for equilibration. The data was collected in triplicate and was found to be accurate within ±0.1 mN m^{-1}. The temperature of the measurement cell was controlled with a Julabo water thermostat within ±0.1 K.

2.2.2. Conductometry. Electrical conductivity of various AAILSs solutions were measured at 298.15 K by a digital conductivity meter (Systronics 308) using a cell of unit cell constant. The temperature of the measurement cell was controlled with a Julabo water thermostat within ±0.1 K. Measurements were performed with an uncertainty of less than 0.5%.

2.2.3. Fluorimetry. Steady-state fluorescence measurements were performed using a Fluorolog (Horiba Jobin Yvon) spectrometer using a quartz cuvette of path length 1 cm. Pyrene was used as the polarity probe, and the emission spectra of pyrene were recorded in the wavelength range 350−500 nm at an excitation wavelength of 334 nm using the excitation and emission slit widths of 1 nm. The concentration of pyrene used was 2 μM. The fluorescence spectra were corrected for the instrumental response. For the aggregation number of the aggregates, steady-state fluorescence quenching measurements were performed using pyrene and cetylpyridinium chloride as probe and quencher, respectively.

2.2.4. Dynamic Light Scattering. The dynamic light scattering measurements (DLS) were performed at 298.15 K on a Zetasizer Nano ZS light scattering apparatus (Malvern Instruments, UK) with a He−Ne laser (633 nm, 4 M_w). ILs solutions of varying concentration were filtered directly into the quart cell using a membrane filter of 0.45 μm pore size. Prior to measurements, the quartz cell was rinsed several times with filtered water and then filled with filtered sample solutions. Temperature of the measurements was controlled with an accuracy of ±0.1 K. Hundred repeated measurements were performed for each sample and average data was considered for analysis. The data evaluation of the dynamic light scattering measurements was performed with the CONTIN algorithm.

2.2.5. Transmission Electron Microscopy. Samples were prepared by putting a drop of AAILS solutions on the carbon-coated copper grid (300 mesh). The residual liquid was blotted immediately. Samples were imaged under a JEOL JEM-2100 electron microscope at a working voltage of 200 kV.

Table 1. Critical Aggregation Concentration (cac), Aggregation Number (N_{agg}), and Hydrodynamic Diameter (D_h) of Various AAILSs in Aqueous Solutions at 298.15 K

AAILSs	cac (mmol kg^{-1}) surf. tension	cac (mmol kg^{-1}) conductometry	cac (mmol kg^{-1}) fluorometry	N_{agg}	D_h (nm)
$GlyC_3LS$	0.74	1.02	0.96	94	1.54
$AlaC_3LS$	0.53	0.81	0.68	81	1.63
$ProC_3LS$	0.48	0.97	0.56	44	1.56
$ValC_3LS$	0.40	0.77	0.82	77	2.08
$GluC_3LS$	0.35	0.41	0.51	72	2.15

3. RESULTS AND DISCUSSION

3.1. Tensiometry. Figure 1 shows the variation of surface tension (γ) as a function of concentration for the various AAILSs at 298.15 K. The γ decreases with the increase in concentration of AAILSs before reaching a critical aggregation concentration (cac), and after that a nearly constant value is obtained. The absence of a minimum around the break point confirms the high purity of compounds. It is shown that the nature of headgroup/alkyl chain length and counterions of the surfactant govern the cac's.[32] More hydrophobic and larger size counterions normally lead to the reduction in cac. The cac values obtained from surface tension measurements for various AAILSs (Table 1) follow the order $GluC_3LS < ValC_3LS < ProC_3LS < AlaC_3LS < GlyC_3LS$. The cac sequence of AAILSs can be correlated to the hydrophobicity and size of the amino acid counterion.[48] $GluC_3LS$ forms aggregates at lower concentration due to the higher hydrophobicity and large hydrodynamic size of $GluC_3$ counterion whereas $GlyC_3LS$ forms aggregates at comparatively higher concentration because of less hydrobhobic and smaller size $GlyC_3$ counterion. The cac's of AAILSs, which range from 0.40 to 0.97 mM, are quite lower as compared to the conventional surfactants having same alkyl chain length and different inorganic or organic counterions, e.g., sodium (8.5 mM), cesium (6.2 mM at 30 °C), tetramethylammonium (5.4 mM), tetraethylammonium (3.7 mM), tetrapropylammonium (2.2 mM), or tetrabutylammonium (1.15 mM).[49,50] The cac's of AAILSs are also lower than those of the ILs based on imidazolium, pyridinium, or pyrrolidinium cations having the same alkyl chain length such as $[C_{12}mim][Br]$ (8.5 mM), $[C_{12}mim][BF_4]$ (7.6 mM), $[C_{12}mim][Cl]$ (13 mM), $[C_{12}mim][CH_3SO_3]$ (14 mM), $[C_{12}Pyr][Br]$ (9.3 mM), or $[C_1C_{12}Pyrr][Br]$ (15 mM).[13,34−37] Large amino acid based counterions are more effective at screening the intramicellar electrostatic repulsion among the polar head groups as compared to small $[Na]^+$, $[Cs]^+$, $[NH_4]^+$, $[Cl]^-$, $[Br]^-$, $[BF_4]^-$, or $[CH_3SO_3]$ counterions, thus allowing significantly lower cac values.

The tensiometric parameters, such as surface tension at cac (γ_{cac}), adsorption efficiency (pC_{20}), surface pressure at cac (Π_{cac}), and minimum surface area per molecule at the air−water interface (A_{min}), are given in Table 2. The γ_{cac} was found to be 25.7, 30.6, 26.0, 27.8, and 27.5 for $AlaC_3LS$, $GluC_3LS$, $GlyC_3LS$, $ProC_3LS$, and $ValC_3Ls$, respectively. The γ_{cac} values indicate that $AlaC_3LS$ is most densely packed at the air−water interface and $GluC_3LS$ is least densely packed. The pC_{20} and Π_{cac} have been determined from the surface tension plots. The pC_{20} is defined as[13,51]

$$pC_{20} = -\log C_{20} \quad (1)$$

Table 2. Surface Tension at cac (γ_{cac}), Adsorption Efficiency (pC_{20}), Effectiveness of Surface Tension Reduction (Π_{cac}), Maximum Surface Excess Concentration (Γ_{max}), and Area of Exclusion Per Monomer (A_{min}), of Various AAILSs at 298.15 K

AAILSs	γ_{cac} (mN m^{-1})	pC_{20}	Π_{cac} (mN m^{-1})	Γ_{max} (μmol m^{-2})	A_{min} (Å^2)
$GlyC_3LS$	26.0	4.4	46.0	1.14	146.0
$ProC_3LS$	27.8	4.6	44.2	1.74	95.5
$AlaC_3LS$	25.7	4.8	46.3	1.24	133.6
$ValC_3LS$	27.5	4.6	44.5	1.61	103.9
$GluC_3LS$	30.6	4.7	41.4	1.75	94.6

where C is the surfactant molar concentration and C_{20} stands for the concentration required to reduce the surface tension of pure solvent by 20 mN m^{-1}. C_{20} is the minimum concentration needed to lead to a saturation of the surface adsorption. Thus, C_{20} can be used as a measure of the efficiency of the surfactant adsorption at the air−water interface.[13,52] Higher pC_{20} value is indicative of higher adsorption efficiency of the surfactant. The Π_{cac}, which is known as surface pressure at cac, is defined as

$$\Pi_{cac} = \gamma_0 - \gamma_{cac} \quad (2)$$

where γ_0 is the surface tension of pure water and γ_{cac} is the surface tension at cac. Both the pC_{20} and Π_{cac} thus obtained are listed in Table 2. The values of pC_{20} and Π_{cac} for various AAILSs are larger as compared to those of analogous conventional ionic surfactants and imidazolium-based ILs, and follow the order AAILSs > imidazolium-based ILs > conventional ionic surfactants,[13,52] showing the superior surface activity of the AAILSs over imidazolium-based ILs or conventional ionic surfactants of the same alkyl chain length. The minimum surface area per molecule (A_{min}), at the air−water interface, which shows the effectiveness of surfactant in populating the air−water interface is calculated using the Gibbs adsorption isotherm and is provided in Table 2.[53] The A_{min} for AAILSs follow the order $GluC_3LS < ProC_3LS < ValC_3LS < AlaC_3LS < GlyC_3LS$, which is according to the hydrophobicity of the amino acid counterions being highest for $GluC_3$ and lowest for $GlyC_3$.

3.2. Conductometry. Figure 2a shows the conductometric profiles of various AAILSs at 298.15 K. The increase of conductivity with concentration, which is observed for dilute solutions, is a direct result of the increasing number of free ions in solution. For all the investigated AAILSs, the conductivity profiles fit into two straight lines with different slopes originating from micellization. The concentration corresponding to the intersection of two straight lines depicts the cac. The values of cac estimated from the electrical conductivity measurements are given in Table 1. Considering the fact that different physical techniques detect different stages of micellization, the cac derived from the different methods is in fairly good agreement.

The temperature dependence of conductivity for a representative AAILS ($GluC_3LS$) is shown in Figure 2b. For other AAILSs, the temperature-dependent conductivity profiles are given in Supporting Information. As is obvious, the conductivity was found to increase with the rise of temperature for all the AAILSs. The cac's were also found to increase with temperature for all the AAILSs except for $GlyC_3LS$ (Table 3). The decrease in slope in the conductivity profiles after cac implies the lower mobility of micelle as compared to free ions in the solution. The counterion binding (β) at the micellar surface in the Stern layer at and after cac results in the decrease in available current carriers, and decreases

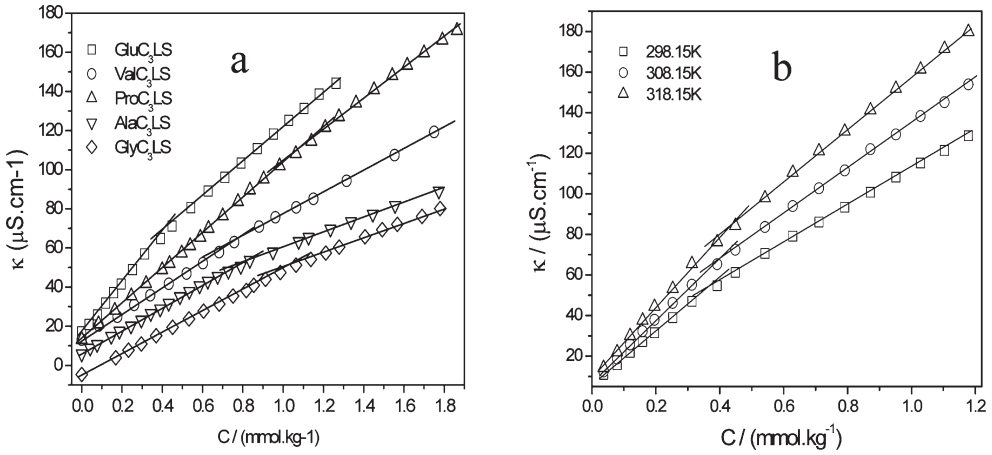

Figure 2. (a) Conductance (κ) of aqueous solutions of various AAILSs as a function of concentration at 298.15 K. The intersection of two straight lines depicts the cac. Data is vertically shifted for better clarity. (b) Temperature-dependent conductivity profile of a representative AAILS ($GluC_3LS$).

Table 3. Critical Aggregation Concentration (cac), Free Energy of Aggregation (ΔG^0_{agg}), Enthalpy of Aggregation (ΔH^0_{agg}), Entropy of Aggregation (ΔS^0_{agg}), and Degree of Counterion Binding (β) of Various AAILSs at Different Temperatures

AAILSs	T (K)	cac (mmol kg^{-1})	ΔG^0_{agg} (kJ mol^{-1})	ΔH^0_{agg} (kJ mol^{-1})	ΔS^0_{agg} (J mol^{-1})	β
$GlyC_3LS$	298.15	1.02	−31.6	−8.0	80.2	0.17
	308.15	0.93	−32.7	−8.5	79.6	0.16
	318.15	0.84	−33.5	−8.8	78.3	0.14
$ProC_3\Lambda S$	298.15	0.97	−32.3	−7.8	82.1	0.19
	308.15	1.07	−32.0	−8.1	77.6	0.15
	318.15	1.15	−32.2	−8.5	74.7	0.13
$AlaC_3LS$	298.15	0.81	−34.5	−8.2	88.1	0.25
	308.15	0.88	−34.3	−8.5	83.6	0.21
	318.15	1.01	−34.1	−8.9	79.3	0.18
$ValC_3LS$	298.15	0.77	−35.2	−8.4	90.1	0.27
	308.15	0.87	−35.7	−8.9	87.1	0.26
	318.15	0.94	−36.0	−9.3	84.0	0.24
$GluC_3LS$	298.15	0.35	−38.9	−8.6	101.5	0.31
	308.15	0.40	−40.4	−9.4	100.6	0.33
	318.15	0.44	−41.3	−10.0	98.5	0.33

the solution conductivity. The ratio of the slope of the linear fragments above and below the cac gives an estimate of β. The values of β thus obtained by a least-squares analysis follow the order $GlyC_3LS < ProC_3LS < AlaC_3LS < ValC_3LS < GluC_3LS$ (Table 3). The β value is associated with the size of the micelle, charge density, and hydrophobic character of the counterion. It is reported that the larger micelles with higher hydrophobicity have a greater tendency to attract counterions than the smaller ones.[54,55] The β varies according to the size of the AAILSs micelles.

The standard Gibbs energy of aggregation (ΔG^0_{agg}), for various AAILSs at different temperatures was derived according to pseudo phase model of micellization:[56,57]

$$\Delta G^0_{agg} = (1 + \beta)RT \ln X_{cac} \quad (3)$$

where X_{cac} is the critical aggregation concentration expressed in mole fraction scale. The estimated values of ΔG^0_{agg} for the AAILSs are reported in Table 3. Significant negative free energy is indicative of spontaneous aggregation of AAILSs. As expected, ΔG^0_{agg} is more negative for the AAILSs having larger counterions. The ΔG^0_{agg} of AAILSs is comparable to that of analogous imidazolium based ILs and SLS.[13,49] Enthalpy of aggregation (ΔH^0_{agg}) was calculated using eq 4, derived from the Gibbs−Helmholtz relation.

$$\Delta H^0_{agg} = -(1 + \beta)RT^2\left(\frac{\partial \ln X_{cac}}{\partial T}\right)_p \quad (4)$$

The entropy of aggregation (ΔS^0_{agg}), was derived using eqs 3 and 4 using the following equation:

$$\Delta S^0_{agg} = \frac{(\Delta H^0_{agg} - \Delta G^0_{agg})}{T} \quad (5)$$

The values of ΔH^0_{agg} and ΔS^0_{agg} are reported in Table 3. The aggregation process usually leads to a positive entropy change, which is mainly due to the melting of the "flickering cluster" that arises out of the hydrophobic effect of amphiphilic part of the surfactant molecules.[58] During aggregation, the endothermic melting of the ordered polar solvent molecules around the nonpolar tail of AAILSs is greater than the subsequent exothermic association of the molecules leading to the positive entropy change. Size and the hydration of the counterions are also responsible for the variation in

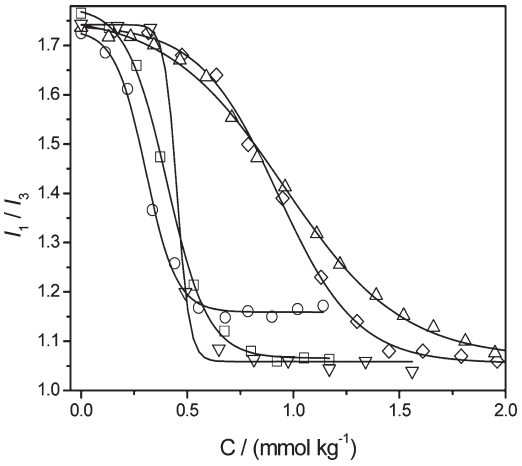

Figure 3. Relative intensities of vibronic bands (I_1/I_3) of pyrene fluorescence in various aqueous solutions of AAILSs: (□) $AlaC_3LS$, (○) $GluC_3LS$, (△) $GlyC_3LS$, (▽) $ProC_3LS$, and (◇) $ValC_3LS$.

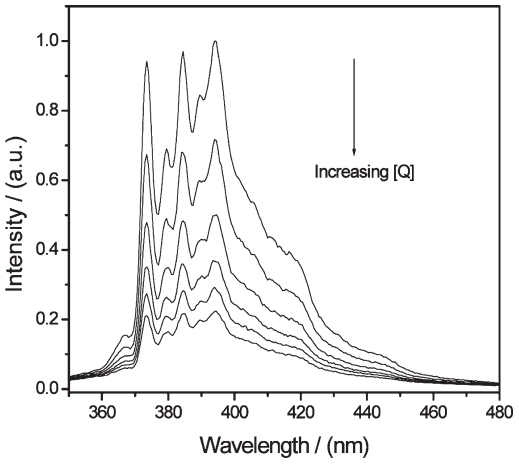

Figure 4. Variation of the emission spectra intensity of 1×10^{-6} mol L^{-1} pyrene in aqueous solutions of a representative AAILS ($ProC_3LS$, 5 mmol kg^{-1}) as a function of the quencher concentration.

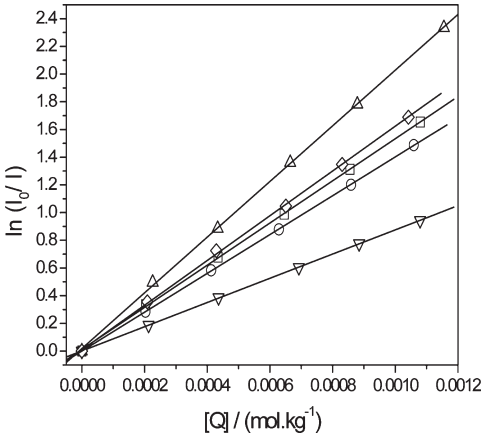

Figure 5. Linear plot of $\ln(I/I_0)$ for 1×10^{-6} mol L^{-1} pyrene in aqueous solutions of various AAILSs: (□) $ValC_3LS$, (○) $GluC_3LS$, (△) $GlyC_3LS$, (▽) $ProC_3LS$, and (◇) $AlaC_3LS$ as a function of cetylpyridinium chloride concentration.

the thermodynamic parameters as is the case for the investigated AAILSs where nonpolar tail is common and changes are observed because of the variation in hydrophobicity and size of amino acid counterions. The AAILS with bigger size and more hydrophobic counterion such as $GluC_3LS$ have very high ΔS^0_{agg} (101.49 J mol^{-1}) as compared to that of relatively smaller size and less hydrophobic $GlyC_3LS$ (80.24 J mol^{-1}). Unlike small inorganic counterion surfactants of the same chain length where the aggregation process is enthalpy driven,[59] the aggregation of AAILSs is primarily driven by the entropic contribution in the studied temperature range of 298.15−318.15 K.

3.3. Fluorimetry. Steady-state fluorescence spectroscopy was used to determine the cac and the microenvironment of the aggregates of various AAILSs in the aqueous solutions. Relative intensities of the vibronic bands (I_1/I_3) of pyrene fluorescence in the aqueous solutions of various AAILSs as a function of concentration are plotted in Figure 3. The ratio I_1/I_3 remains constant initially and then decreases rapidly until cac is reached. After cac, the I_1/I_3 becomes almost constant with further increase in the concentration of AAILSs. The cac derived from the I_1/I_3 data is given in Table 1 and is compared with the values obtained from tensiometry and conductometry. The vibronic structure of the fluorescence spectrum of monomeric pyrene is known to be sensitive to the local polarity. The ratio I_1/I_3 of micelle-solubilized pyrene increases on going toward the more polar solvents.[57] I_1/I_3 values for the AAILSs lie in the range of 1.06−1.16, which is quite comparable with the conventional surfactants, for example, sodium lauryl sulfate (1.14).[60] For the pyrene solvated in nonpolar solvents like toluene the characteristic value of I_1/I_3 is 1.11.[60] Therefore, from I_1/I_3 values for the AAILSs, it can be safely concluded that the pyrene has been solubilized in the core of aggregates and experiences a highly nonpolar environment.

3.3.1. Aggregation Number. The steady-state fluorescence quenching technique was used to determine the aggregation number (N_{agg}) of AAILSs. The equilibrium of the AAILSs between the aqueous and aggregation phases follows the Poisson distribution. The following equation is applied to fluorescence quenching data:[61]

$$\ln I = \ln I_0 - C_q/C_a = \ln I_0 - N_{agg}C_q/(C_t - \text{cac}) \qquad (6)$$

where C_q, C_a, and C_t are the concentrations of quencher, aggregate, and total AAILSs, respectively, while I and I_0 are the fluorescence intensities in the presence and absence of quencher. Figure 4 shows the emission spectra of pyrene in aqueous solutions of a representative AAILS ($ProC_3LS$) in the presence of varying quencher concentrations. The emission intensity of pyrene decreases with the increase of quencher concentration. Figure 5 shows the plot of $\ln(I/I_0)$ against C_q for various AAILSs. Using the slope of these linear plots and cac, the N_{agg} was determined by using the eq 6. The N_{agg} for various AAILSs varies in the order $ProC_3LS$ < $GluC_3LS$ < $ValC_3LS$ < $AlaC_3LS$ < $GlyC_3LS$ (Table 1). The hydrodynamic diameter (D_h) of the aggregates of various AAILSs at a solution concentration of 5 mmol kg^{-1} (∼5 times the cac) was measured from dynamic light scattering (DLS) measurements. The CONTIN plots corresponding to the radii distribution functions for various AAILSs aggregates are shown in Figure 6. DLS data show a single micellar distribution with an average D_h ranging from ∼1.5 to 2 nm. The self-assembled structures of AAILSs were imaged through TEM (Figure 7). TEM micrographs show uniformly distributed spherical-shaped aggregates of ∼3−4 nm size, which is consistent with the size observed from DLS measurements.

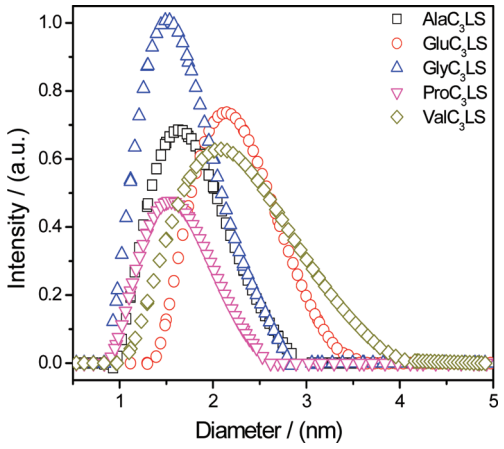

Figure 6. Size distribution of aggregates of various AAILSs in aqueous media from DLS measurements. The concentration of each solution was 5 mmol kg^{-1}.

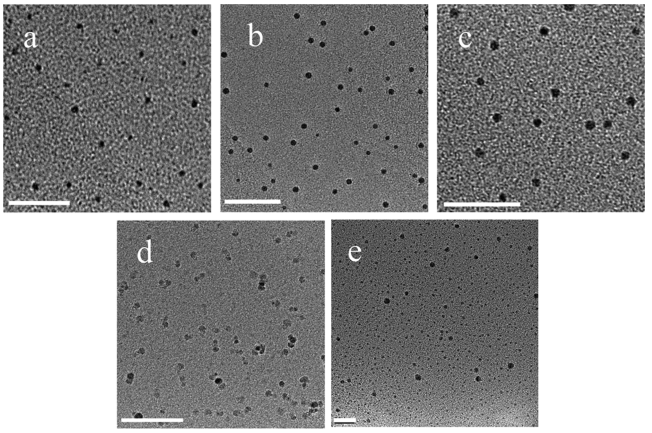

Figure 7. TEM images of aggregates of AAILSs (a) $AlaC_3LS$, (b) $GluC_3LS$, (c) $GlyC_3LS$, (d) $ProC_3LS$, and (e) $ValC_3LS$ in aqueous media. Bar represents 20 nm. The concentration of each solution was 5 mmol kg^{-1}.

4. CONCLUSIONS

Aggregation characteristics of amino acid ionic liquid surfactants (AAILSs) have been examined in aqueous media through a variety of physical and spectroscopic techniques. Because of comparable size and hydrophobicity, the cac's of AAILSs are nearly same. The cac of AAILS was found much lower as compared to the conventional ionic surfactants or analogous imidazolium-based ILs of the same alkyl chain length due to large size and high hydrophobicity of amino acid counterions. Aggregation process in AAILSs was found to be governed by the entropic parameter. Aggregation number and aggregate size of AAILSs were found to depend on the structure of counterion amino acid. AAILSs with bigger counterions formed larger aggregates with lesser aggregation number.

■ ASSOCIATED CONTENT

Supporting Information. Chemical analysis of synthesized AAILSs and temperature-dependent conductivity measurements are provided. This material is available free of charge via the Internet at http://pubs.acs.org.

■ AUTHOR INFORMATION

Corresponding Author

*Tel.: +91-278-2567039. Fax: +91-278-256 7562/256 6970. E-mail: mailme_arvind@yahoo.com, arvind@csmcri.org.

■ ACKNOWLEDGMENT

The authors are thankful to the Department of Science and Technology (DST), Government of India, for financial support for this work (No. SR/S/PC-55/2008 and SR/S/PC-4/2010).

■ REFERENCES

(1) Earle, M. J.; McCormac, P. B.; Seddon, K. R. *Chem. Commun.* **1998**, 2245.
(2) Welton, T. *Chem. Rev.* **1999**, *99*, 2071.
(3) Holbrey, J. D.; Seddon, K. R. *Clean Prod. Processes* **1999**, *1*, 223.
(4) Wasserscheid, P.; Keim, W. *Angew. Chem., Int. Ed.* **2000**, *39*, 3772.
(5) Anderson, J. L.; Ding, J.; Welton, T; Armstrong, D. W. J. *Am. Chem. Soc.* **2002**, *124*, 14247.
(6) Rogers, R. D.; Seddon, K. R. *Science* **2003**, *302*, 792.
(7) Seddon, K. R. *Nature Mater.* **2003**, *2*, 363.
(8) *Ionic Liquids in Synthesis*; Wasserscheid, P., Welton, T., Eds.; Wiley: New York, 2003.
(9) Earle, M. J.; Esperanca, J. M. S. S.; Gilea, M. A.; Canongia Lopes, J. N.; Rebelo, L. P. N.; Magee, J. W.; Seddon, K. R.; Widergren, J. A. *Nature* **2006**, *439*, 831.
(10) Santos, L. M. N. B. F.; Lopes, J. N. C.; Coutinho, J. A. P.; Esperancüa, J. M. S. S.; Gomes, L. R.; Marrucho, I. M.; Rebelo, L. P. N. *J. Am. Chem. Soc.* **2007**, *129*, 284.
(11) Singh, T.; Kumar, A. *J. Phys. Chem. B* **2008**, *112*, 4079.
(12) Singh, T.; Kumar, A. *Colloids Surf. A* **2008**, *318*, 263.
(13) Dong, B.; Li, N.; Zheng, L.; Yu, L.; Inoue, T. *Langmuir* **2007**, *23*, 4178.
(14) Dong, B.; Zhao, X. Y.; Zheng, L. Q.; Zhang, J.; Li, N.; Inoue, T. *Colloids Surf. A* **2008**, *317*, 666.
(15) Goodchild, I.; Collier, L.; Millar, S. L.; Prokeš, I.; Lord, J. C. D.; Butts, C. P.; Bowers, J.; Webster, J. R. P.; Heenan, R. K. *J. Colloid Interface Sci.* **2007**, *307*, 455.
(16) Wang, J.; Wang, H.; Zhang, S.; Zhang, H.; Zhao, Y. *J. Phys. Chem. B* **2007**, *111*, 6181.
(17) Zhao, Y.; Gao, S. J.; Wang, J. J.; Tang, J. M. *J. Phys. Chem. B* **2008**, *112*, 2031.
(18) Bowers, J.; Butts, P.; Martin, J.; Vergara-Gutierrez, C.; Heenan, K. *Langmuir* **2004**, *20*, 2191.
(19) Inoue, T.; Ebina, H.; Dong, B.; Zheng, L. Q. *J. Colloid Interface Sci.* **2007**, *314*, 236.
(20) Bandrés, I.; Meler, S.; Giner, B.; Cea, P.; Lafuente, C. *J. Soln. Chem.* **2009**, *38*, 1622.
(21) Dorbritz, S.; Ruth, W.; Kragl, U. *Adv. Synth. Catal.* **2005**, *347*, 1273.
(22) Miskolczy, Z.; Sebok-Nagy, K.; Biczok, L.; Goektuerk, S. *Chem. Phys. Lett.* **2004**, *400*, 296.
(23) Seth, D.; Sarkar, S.; Sarkar, N. *Langmuir* **2008**, *24*, 7085.
(24) Dong, B.; Gao, Y.; Su, Y.; Zheng, L.; Xu, J.; Inoue, T. *J. Phys. Chem. B* **2010**, *114*, 340.
(25) Dong, B.; Zhang, J.; Zheng, L. Q.; Wang, S. Q.; Li, X. W.; Inoue, T. *J. Colloid Interface Sci.* **2008**, *319*, 338.
(26) Wang, H. Y.; Wang, J. J.; Zhang, S. B.; Xuan, X. P. *J. Phys. Chem. B* **2008**, *112*, 16682.
(27) Blesic, M.; Lopes, A.; Melo, E.; Petrovski, Z.; Plechkova, N. V.; Canongia Lopes, J. N.; Seddon, K. R.; Rebelo, L. P. N. *J. Phys. Chem. B* **2008**, *112*, 8645.
(28) Blesic, M.; Marques, M. H.; Plechkova, N. V.; Seddon, K. R.; Rebelo, L. P. N.; Lopes, A. *Green Chem.* **2007**, *9*, 481.
(29) Łuczak, J.; Hupka, J.; Thöming, J.; Jungnickel, C. *Colloids Surf. A* **2008**, *329*, 125.

(30) Wang, H.; Feng, Q.; Wang, J.; Zhang, H. *J. Phys. Chem. B* **2010**, *114*, 1380.
(31) Wang, J.; Zhang, L.; Wang, H.; Wu, C. *J. Phys. Chem. B* **2011**, *115*, 4955.
(32) Brown, P.; Butts, C.; Dyer, R.; Eastoe, J.; Grill, I.; Guittard, F.; Rogers, S.; Heenan, R. *Langmuir* **2011**, *27*, 4563.
(33) Srinivasa Rao, K.; Singh, T.; Kumar, A. *Langmuir* **2011**, *27*, 9261.
(34) Blesic, M.; Swadzba-Kwasny, M.; Holbrey, J. D.; Canongia Lopes, J. N.; Seddon, K. R.; Rebelo, L. P. N. *Phys. Chem. Chem. Phys.* **2009**, *11*, 4260.
(35) El Seoud, O. A.; Pires, P. A. R.; Abdel-Moghny, T.; Bastos, E. L. *J. Colloid Interface Sci.* **2007**, *313*, 296.
(36) Cornellas, A.; Perez, L.; Comelles, F.; Ribosa, I.; Manresa, A.; Garcia, M. T. *J. Colloid Interface Sci.* **2011**, *355*, 164.
(37) Tariq, M.; Podgorsek, A.; Ferguson, J. L.; Lopes, A.; Costa Gomes, M. F.; Pádua, A. A. H.; Rebelo, L. P. N.; Canongia Lopes, J. N. *J. Colloid Interface Sci.* **2011**, *360*, 606.
(38) Bowlas, C. J.; Bruce, D. W.; Seddon, K. R. *Chem. Commun.* **1996**, 1625.
(39) Gordon, C. M.; Holbrey, J. D.; Kennedy, A. R.; Seddon, K. R. *J. Mater. Chem.* **1998**, *8*, 2627.
(40) Adams, C. J.; Bradley, A. E.; Seddon, K. R. *Aust. J. Chem.* **2001**, *54*, 679.
(41) Zhou, Y.; Antonietti, M. *Chem. Mater.* **2004**, *16*, 544.
(42) Dattelbaum, A. M.; Baker, S. N.; Baker, G. A. *Chem.Commun.* **2005**, 939.
(43) Wang, T.; Kaper, H.; Antonietti, M.; Smarsly, B. *Langmuir* **2007**, *23*, 1489.
(44) Trivedi, T. J.; Srinivasa Rao, K.; Singh, T.; Mandal, S. K.; Sutradhar, N.; Panda, A. B.; Kumar, A. *ChemSusChem* **2011**, *4*, 604.
(45) Seddon, K. R.; Stark, A.; Torres, M. J. *Pure Appl. Chem.* **2000**, *72*, 2275.
(46) Blanchard, L. A.; Gu, Z.; Brennecke, J. F. *J. Phys. Chem. B* **2001**, *105*, 2437.
(47) Vogel, A. I. *A Textbook of Quantitative Inorganic Analysis*, 3rd ed.; Longmans: London, 1961.
(48) Hecht, D.; Tadesse, L.; Walters, L. *J. Am. Chem. Soc.* **1993**, *115*, 3336.
(49) Bakshi, M. S. *Bull. Chem. Soc. Jpn.* **1996**, *69*, 2723.
(50) Benrraou, M.; Bales, B. L.; Zana, R. *J. Phys. Chem. B* **2003**, *107*, 13432.
(51) Rosen, M. J. *Surfactants and Interfacial Phenomena*, 2nd ed.; Wiley: New York, 1989.
(52) Mukerjee, P.; Mysels, K. J. *Critical Micelle Concentrations of Aqueous Surfactant Systems*; U.S. Dept. Commerce, NBS: Washington, DC, 1970.
(53) Jaycock, M. J.; Parfitt, G. D. *Chemistry of Interfaces*; John Wiley and Sons: New York, 1981.
(54) Tsao, H. K. *J. Phys. Chem. B* **1998**, *102*, 10243.
(55) Bhattacharya, S.; Haldar, J. *Langmuir* **2004**, *20*, 7940.
(56) Phillips, J. N. *Trans. Faraday Soc.* **1955**, *51*, 561.
(57) Mehta, S. K.; Bhasin, K. K.; Kumar, A.; Dham, S. *Colloids Surf. A* **2006**, *278*, 17.
(58) Tanford, C. *The Hydrophobic Effect: Formation of Micelles and Biological Membranes*; Wiley: New York, 1980; Vol. 2.
(59) Ropers, M. H.; Czichocki, G.; Brezesinski, G. *J. Phys. Chem. B* **2003**, *107*, 5281.
(60) Kalyanasundaram, K.; Thomas, J. K. *J. Am. Chem. Soc.* **1977**, *99*, 2039.
(61) Turro, N. J.; Yekta, A. *J. Am. Chem. Soc.* **1978**, *100*, 5951.